J Eng Math
DOI 10.1007/s10665-012-9566-9

Analysis of routing protocols and interference-limited communication in large wireless networks via continuum modeling

Nathanial Burch · Edwin K. P. Chong · Don Estep · Jan Hannig

Received: 1 August 2010 / Accepted: 1 June 2012

Abstract The evaluation and assessment of the design of large wireless networks is an important problem in numerous applications. Direct simulation is a traditional approach for studying such networks but is severely limited in its utility as the size of the network increases. This necessitates other means for studying large networks, one of which is the modeling of large networks with continuum models. In this paper, we introduce nonlinear partial differential equations whose solutions approximate the expected behavior of large networks governed by probabilistic communication rules. The relative speed at which solutions can be obtained from the continuum models allows for the investigation of routing protocols and communication limitations due to interference—a feat that is not feasible via simulation methods. Specifically, we investigate the effects of a directed diffusion routing protocol and explore communication limitations in an interference-sensitive network. Network design studies using the approximating continuum models are then presented.

Keywords Continuum modeling · Network design · Stochastic network simulation · Wireless ad hoc networks

N. Burch (✉)
Statistical and Applied Mathematical Sciences Institute, Research Triangle Park, NC 27709, USA
e-mail: burchn@samsi.info

E. K. P. Chong
Department of Electrical and Computer Engineering, Colorado State University, Fort Collins, CO 80523, USA
e-mail: edwin.chong@colostate.edu

D. Estep
Department of Statistics, Colorado State University, Fort Collins, CO 80523, USA
e-mail: estep@stat.colostate.edu

E. K. P. Chong · D. Estep
Department of Mathematics, Colorado State University, Fort Collins, CO 80523, USA

J. Hannig
Department of Statistics and Operations Research, University of North Carolina at Chapel Hill, Chapel Hill, NC 27599, USA
e-mail: jan.hannig@unc.edu

Published online: 29 August 2012

1 Introduction

The goal of this paper is to model the propagation of data through a large network consisting of transmitters and receivers located at nodes arranged in a one- or two-dimensional grid, where each device communicates according to probabilistic communication rules with its two or four immediate neighbors, respectively. The devices are limited in power, bandwidth, and storage space, whereas the communication is limited by interference from the environment and from other devices sharing the same wireless channel. To model these unique characteristics, a stochastic description of the network and communication rules is used. Direct simulation and statistical analysis of large networks is expensive, and consequently, the use of other approaches, e.g., continuum models, to approximate statistics of the network while avoiding direct simulation is necessary. In [1], one such approach is considered that employs the so-called fluid approach by representing the large-scale sensor network with continuous entities, e.g., sensor and traffic densities. In previous work [2], we derive partial differential equations (PDEs) whose solutions approximate the expected value of the queue lengths throughout the network. Since this approach avoids the simulation of multiple networks, sensitivity analyses, network optimization studies, and design studies can be performed with minimal computational cost.

Sensor networks have revolutionized data gathering in many applications [3], as predicted in [4]. For the example of a network of sensors deployed along a volcano, collecting large quantities of data to monitor seismic and infrasonic activity, where data are transmitted from device to device until finally delivered to the base station, see [5,6]. Similarly, see [7] for a large network of wireless sensors installed in a redwood tree to collect data such as air temperature and solar radiation at fixed time increments. Each of these networks encounters challenges with data collection and transmission of that data out of the network. The design of such networks is crucial so that, for instance, the collected data are successfully transmitted out of the network. For comprehensive reviews of sensor networks, subsequent engineering challenges, and a more complete list of applications of sensor networks, e.g., military and health applications, we refer the reader to [3,4,8,9].

Understanding the characteristics and properties of such networks is vital for design and deployment. In [10], transport capacities of networks as the number of devices increase, i.e., the network becomes dense in space, are investigated. Optimal strategies for deploying sensors in a large-scale sensor network have been studied in [11,12]. Direct simulation of networks with a large number of wireless devices may be used to generate statistical descriptions of the network, e.g., packet reception and communication range, see [13]. Further, studies of throughput, capacity, and performance are found in [14–17]. The impact of interference on the throughput in a multihop wireless network was investigated in [18] via conflict graphs.

In comparatively few instances, continuum models have been used to study wireless networks. A reaction–diffusion PDE is derived in [19] to model the wavefront behavior of an epidemic traveling through a network. The work of [20,21] used a set of PDEs to determine routing strategies that increased the throughput of the system and the energy efficiency of the network. In [22], a continuum of network nodes is used to approximate a dense network and information flow through the resulting continuum of nodes is optimized. In our previous research [2], a nonlinear PDE is derived whose solution approximates the expected queue for a large wireless network obeying simple communication rules. A convergence proof to complement the work of [2] is presented in [23].

The contribution of this paper is to present continuum models that approximate the expected normalized queue length in a large network and allow for a general class of communication and interference protocols. This work extends the modeling approach considered in [2] to include a large class of networks with diverse sets of communication protocols. Understanding the effects of altering the communication protocol is critical in the design of wireless networks. With these examples, we illustrate that the continuum modeling approach provides an efficient means for analyzing the effects of varying the routing protocol and transmission interference. Such analysis can then be used to make informed decisions about the design of the network and its components. In particular, we study the effects of both routing and interference protocols on the expected normalized queue lengths in large networks. This approach overcomes the computational burden associated with many other approaches and allows for network design studies.

The rest of this paper is organized as follows. In Sect. 2, we present models for discrete networks in one dimension, while introducing notation and modeling assumptions. An important statistic of networks, the expected normalized queue length, is shown to solve a difference equation. Section 3 presents assumptions as the number of devices increases so that the difference equation converges to a PDE continuum model. In Sect. 4, we extend the modeling approach to two dimensions. Section 5 demonstrates the utility of using continuum models as an aid in the study and design of large networks.

2 One-dimensional discrete stochastic network model

In this section, we present a model for a network of wireless communication devices behaving according to a set of probabilistic communication rules. We assume that the wireless sensors (nodes) are uniformly located on a grid and transmit data through the network via communication between adjacent nodes. The communication rules are probabilistic and incorporate probabilities of whether a node decides to transmit or receive, the direction chosen for subsequent transmissions, and interference from other transmitting nodes. The devices generate data at predetermined time increments and then store the data in a queue. Specialized receiving nodes, e.g., communication relay devices that transmit to a computer, are located on the boundary of the network. The job of the network is to transmit the sensor data to such specialized devices and, consequently, out of the network.

We consider a homogeneous array of N interior nodes; i.e., transmission, interference, storage capacity, etc. do not explicitly depend on the node $n \in \{1, \ldots, N\}$. Due to storage limitations, each device is capable of storing at most Q^* data in its queue. We then define $\widetilde{Q}(k, n)$, $k = 0, 1, \ldots, T$, to be the *normalized* queue length of node n's queue at time step k; i.e., $\widetilde{Q}(k, n)$ is the number of data in node n's queue at time step k divided by Q^*. The *expected* normalized queue length is denoted by $Q(k, n)$. The network begins with a known initial normalized queue length $\widetilde{Q}(0, n) = Q_0(n)$. At each time step, node n receives a random number of data, $\widetilde{G}(k, n)$, following a nonnegative, discrete distribution with mean $G(k, n)$, and stores the data in its queue. A natural choice for the distribution of $\widetilde{G}(k, n)$ is that of a Poisson random variable. With probability $F(n, Q(k, n))$, independent of the other nodes, node n elects whether to be a transmitting node. We assume F is monotone in the second variable, $F(n, 0) = 0$, and $F(n, 1) = 1$. These assumptions are tantamount to specifying that the probability of transmission from a node with an empty queue is zero and that from a node with a full queue is one. The nodes that do not elect to transmit are designated to be receiving nodes. The transmitting nodes then decide on an intended receiver by selecting a direction of transmission; i.e., the probability that node n transmits to node $n \pm 1$ is $B^k_{n,n\pm1}$. Note that $B^k_{n,n+1} + B^k_{n,n-1} = 1$ and $B^k_{n,n\pm1} \in [0, 1]$. Finally, a transmission from a transmitting node n to a receiving node $n \pm 1$ is successful, i.e., there is no interference, with probability $1 - I^k_{n,n\pm1}$. The interference probability $I^k_{n,n\pm1}$ models all factors contributing to interference, e.g., other transmitting devices, limited power, and the environment, in aggregate. Consequently, detailed effects of fading, shadowing, and power adaptation are not specifically modeled. Both $B^k_{n,n\pm1}$ and $I^k_{n,n\pm1}$ may depend on n, $Q(k, n)$, and on the expected normalized queue length at nearby nodes, but do not depend explicitly on time. The choice for F, $B^k_{n,n\pm1}$, and $I^k_{n,n\pm1}$ to depend on the expected normalized queue length $Q(k, n)$, rather than $\widetilde{Q}(k, n)$ for example, requires justification and is discussed in detail in Sect. 2.1.

The notation hereafter is cumbersome so we introduce a superscript k to denote the time step and a subscript n to denote the node. With this notation and the previous description of the network, a transmission from node n to node $n \pm 1$ is successful with probability

$$F^k_n B^k_{n,n\pm1}\left(1 - F^k_{n\pm1}\right)\left(1 - I^k_{n,n\pm1}\right),$$

and from node $n \pm 1$ to node n is successful with probability

$$\left(1 - F^k_n\right) B^k_{n\pm1,n} F^k_{n\pm1}\left(1 - I^k_{n\pm1,n}\right).$$

Together, these give rise to the Markov process for the vector of normalized queue lengths

$$\widetilde{Q}_n^{k+1} = \begin{cases} \widetilde{Q}_n^k + \frac{1}{Q^*} + \frac{\widetilde{G}_n^k}{Q^*} & \text{with probability} \\ \quad \left(1 - F_n^k\right) B_{n-1,n}^k F_{n-1}^k \left(1 - I_{n-1,n}^k\right) + \left(1 - F_n^k\right) B_{n+1,n}^k F_{n+1}^k \left(1 - I_{n+1,n}^k\right), \\ \widetilde{Q}_n^k - \frac{1}{Q^*} + \frac{\widetilde{G}_n^k}{Q^*} & \text{with probability} \\ \quad F_n^k B_{n,n+1}^k \left(1 - F_{n+1}^k\right) \left(1 - I_{n,n+1}^k\right) + F_n^k B_{n,n-1}^k \left(1 - F_{n-1}^k\right) \left(1 - I_{n,n-1}^k\right), \\ \widetilde{Q}_n^k + \frac{\widetilde{G}_n^k}{Q^*} & \text{otherwise.} \end{cases} \tag{1}$$

The boundary nodes $n = 0$ and $n = N + 1$ are specialized devices on the boundary of the network. A *sink* boundary node has a direct connection to the final user and therefore receives all data transmitted to it, immediately transmitting them out of the network. A *wall* boundary node, on the other hand does not have a connection to the final user, i.e., such boundary nodes neither accept nor send transmissions. For clarity, we postpone further discussion to Sect. 2.2, where we give it full consideration.

2.1 Network simulation algorithm

The described communication protocols, interference rules, and boundary behaviors are now presented in an algorithm for simultaneously simulating M wireless networks. We let $\widetilde{Q}_n^{k,m}$ denote the normalized queue length at node n and time step k for network m.

Recall that F_n^k, $B_{n,n+1}^k$, and $I_{n,n\pm1}^k$ each depend on the expected normalized queue length Q_n^k. This dependence assumption on Q_n^k, rather than $\widetilde{Q}_n^k$ for example, is made purely for mathematical convenience so that an expectation of (1) can easily be taken. Since Q_n^k is unknown a priori, however, we must approximate it in order to simulate the networks described by (1). The paper [2] investigates two such approximations, namely the *instantaneous* normalized queue length $\widetilde{Q}_n^k$ and the *average* normalized queue length across M simultaneous network simulations. An actual network is likely to have its transmission protocols depend on $\widetilde{Q}_n^k$, and a convergence proof for this case is given in [23] for the one-dimensional network considered in [2]. In this paper, we approximate Q_n^k with the average normalized queue length across M simultaneous simulations,

$$\bar{Q}_n^{k,M} = \frac{1}{M} \sum_{m=1}^{M} \widehat{Q}_n^{k,m}, \tag{2}$$

where $\widehat{Q}_n^{k,m}$ follows the Markov process

$$\widehat{Q}_n^{k+1,m} = \begin{cases} \widehat{Q}_n^{k,m} + \frac{1}{Q^*} + \frac{\widetilde{G}_n^k}{Q^*} & \text{with probability} \\ \quad \left(1 - \bar{F}_n^k\right) \bar{B}_{n-1,n}^k \bar{F}_{n-1}^k \left(1 - \bar{I}_{n-1,n}^k\right) + \left(1 - \bar{F}_n^k\right) \bar{B}_{n+1,n}^k \bar{F}_{n+1}^k \left(1 - \bar{I}_{n+1,n}^k\right), \\ \widehat{Q}_n^{k,m} - \frac{1}{Q^*} + \frac{\widetilde{G}_n^k}{Q^*} & \text{with probability} \\ \quad \bar{F}_n^k \bar{B}_{n,n+1}^k \left(1 - \bar{F}_{n+1}^k\right) \left(1 - \bar{I}_{n,n+1}^k\right) + \bar{F}_n^k \bar{B}_{n,n-1}^k \left(1 - \bar{F}_{n-1}^k\right) \left(1 - \bar{I}_{n,n-1}^k\right), \\ \widehat{Q}_n^{k,m} + \frac{\widetilde{G}_n^k}{Q^*} & \text{otherwise.} \end{cases} \tag{3}$$

The bar notation in (3) represents using (2) in place of Q_n^k, e.g., if $F_n^k = \sin(\frac{\pi}{2} Q_n^k)$, then $\overline{F}_n^k = \sin(\frac{\pi}{2} \overline{Q}_n^{k,M})$. We remark that the use of the approximation (2) is tantamount to perturbing the state transition rules in the Markov process. We present an outline of an algorithm for simulating the Markov process (3) in Algorithm 1.

Algorithm 1: Simulating M one-dimensional networks with N interior nodes

specify the network parameters, e.g., F_n^k, $B_{n,n\pm1}^k$, G_n^k, Q_0, and Q^*
initialize the M networks with $\widehat{Q}_n^{0,m} = Q_0(n)$, for all m, n
for $k = 0, \ldots, T-1$ *(number of time steps)* **do**
  compute $\overline{Q}_n^{k,M}$
  for $m = 1, \ldots, M$ *(number of networks)* **do**
    for $n = 1, \ldots, N$ *(number of interior nodes)* **do**
      $\widehat{Q}_n^{k+1,m} = \widehat{Q}_n^{k,m} + \frac{\widetilde{G}_n^{k,m}}{Q^*}$ *(new data have been generated)*
      determine if node n is a transmitting node via $\overline{F}_n^k$
      determine the direction of intended transmission via $\overline{B}_{n,n\pm1}^k$
    end
    for $n = 0, \ldots, N+1$ *(number of nodes)* **do**
      for $j = 1, \ldots, N$ *(number of interior nodes)* **do**
        if *node j transmits to node n successfully* **then**
          $\widehat{Q}_n^{k+1,m} = \widehat{Q}_n^{k+1,m} + \frac{1}{Q^*}$
          $\widehat{Q}_j^{k+1,m} = \widehat{Q}_j^{k+1,m} - \frac{1}{Q^*}$
        end
      end
    end
  end
end

Since the approximation (2) perturbs the state transition probabilities in (1) to those in (3), it is not immediately obvious whether Q_n^k is approximated from averages of simulations according to Algorithm 1. The simulations in both this paper and [2] show convincing evidence of this, and on one hand, it is natural to believe that $\overline{Q}_n^{k,M}$ approximates Q_n^k since, for sufficiently large M, $\overline{F}_n^k \approx F_n^k$, $\overline{B}_{n,n+1}^k \approx B_{n,n+1}^k$, and $\overline{I}_{n,n\pm1}^k \approx I_{n,n\pm1}^k$. On the other hand, determining precise conditions to guarantee a specific type of convergence of (3) to (1) is not clear. Obtaining such convergence results is an open problem and out of the scope of this paper.

2.2 The expected normalized queue length and specialized network models

The focus of this paper is on the expected normalized queue length, which may be approximated from the simulations as in (2). The expected normalized queue length describes so-called macroflow behavior of the network. We now demonstrate that the expected normalized queue length is the solution to a difference equation. Taking an expectation of the Markov process (1) yields the difference equation for $k \in \{0, 1, \ldots\}$ and $n \in \{1, \ldots, N\}$

$$\begin{cases} Q_n^{k+1} = Q_n^k + \dfrac{G_n^k}{Q^*} + \dfrac{1}{Q^*}\left(1 - F_n^k\right)\left\{B_{n-1,n}^k F_{n-1}^k \left(1 - I_{n-1,n}^k\right) + B_{n+1,n}^k F_{n+1}^k \left(1 - I_{n+1,n}^k\right)\right\} \\ \qquad\qquad - \dfrac{1}{Q^*} F_n^k \left\{B_{n,n+1}^k \left(1 - F_{n+1}^k\right)\left(1 - I_{n,n+1}^k\right) + B_{n,n-1}^k \left(1 - F_{n-1}^k\right)\left(1 - I_{n,n-1}^k\right)\right\} \\ Q_n^0 = Q_0(n). \end{cases} \tag{4}$$

We now explain in detail the effects of the boundary nodes on the interior nodes. To do this, we consider a one-dimensional network of nodes with a sink located at the left boundary and a wall at the right boundary (Fig. 1).

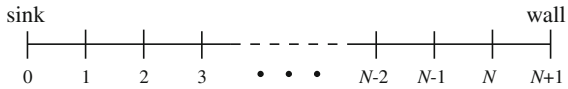

Fig. 1 A one-dimensional network of nodes with a sink located at the *left boundary* and a wall at the *right boundary*

Then, for node 1, which is located directly to the right of the sink, since $F_0^k = 0$,

$$Q_1^{k+1} = Q_1^k + \frac{G_1^k}{Q^*} + \frac{1}{Q^*}\left(1-F_1^k\right) B_{2,1}^k F_2^k \left(1-I_{2,1}^k\right) - \frac{1}{Q^*} F_1^k \left\{B_{1,2}^k \left(1-F_2^k\right)\left(1-I_{1,2}^k\right) + B_{1,0}^k \left(1-I_{1,0}^k\right)\right\}. \tag{5}$$

For node N, which is located directly to the left of the wall, since $F_{N+1}^k = 0$ and $I_{N,N+1}^k = 1$,

$$Q_N^{k+1} = Q_N^k + \frac{G_N^k}{Q^*} + \frac{1}{Q^*}\left(1-F_N^k\right) B_{N-1,N}^k F_{N-1}^k \left(1-I_{N-1,N}^k\right) - \frac{1}{Q^*} F_N^k B_{N,N-1}^k \left(1-F_{N-1}^k\right)\left(1-I_{N,N-1}^k\right). \tag{6}$$

To illustrate how routing and interference protocols are incorporated into the network model, we consider three different network models. The first is a relatively simple model with constant routing bias and constant probability of interference presented largely for illustration purposes. The second incorporates interference via a two-step interference protocol [14,18], which is a second-order approximation of the power-law model for interference. The third uses local information to transmit packets in the direction of the neighbor with lower expected queue, which is a special case of the directed diffusion model [4].

Network 1 (Simple model) We begin with a description of a simple network in order to familiarize the reader with the approach that will be used for more sophisticated network protocols. We assume the direction of transmission is determined by

$$B_{n,n+1}^k = \frac{1}{2} + b_0 \Delta x, \quad b_0 \in \mathbb{R}, \quad \forall n, k, \tag{7a}$$

where Δx is the distance between two neighboring nodes. In (7a), the parameter b_0 represents a bias in transmission, e.g., if $b_0 > 0$, then there is a bias to transmit to the right more frequently. We assume $b_0 \Delta x \in [-1/2, 1/2]$. The interference protocol is given by

$$1 - I_{n,n\pm1}^k = c, \quad c \in (0, 1], \quad \forall n, k. \tag{7b}$$

Inserting (7a) and (7b) into (4) and performing tedious algebraic manipulations gives

$$Q_n^{k+1} = Q_n^k + \frac{G_n^k}{Q^*} + \frac{c}{2Q^*}\left(F_{n-1}^k - 2F_n^k + F_{n+1}^k\right) + \frac{b_0 c \Delta x}{Q^*}\left(1 - 2F_n^k\right)\left(F_{n-1}^k - F_{n+1}^k\right). \tag{8}$$

Network 2 (Protocol interference model) Since signal strength decreases, according to a power-law decay, as distance of transmission increases, a node that is not an immediate neighbor of the intended receiver may still be able to interfere with the transmission. For this model, we assume

$$B_{n,n+1}^k = \frac{1}{2} + b_n^k \Delta x \tag{9a}$$

and

$$1 - I_{n,n\pm1}^k = \left(1 - F_{n\pm2}^k\right)\left(1 - \beta F_{n\pm3}^k\right)\left(1 - \beta F_{n\mp1}^k\right), \quad \beta \in [0, 1], \quad \forall n, k. \tag{9b}$$

The assumption (9b) incorporates an additional source of interference, i.e., a probabilistic interference (with probability β) from *transmitting* nodes that are two steps away from the intended receiver. The parameter β can be chosen to model channel and transmission power and incorporate external sources of interference as well. Inserting (9a) and (9b) into (4) gives

$$
\begin{aligned}
Q_n^{k+1} = Q_n^k + \frac{G_n^k}{Q^*} + \frac{1}{2Q^*} \Big\{ & \left(1-F_n^k\right)\left(F_{n-1}^k\left(1-F_{n+1}^k\right)\left(1-\beta F_{n+2}^k\right)\left(1-\beta F_{n-2}^k\right)\right. \\
& + F_{n+1}^k\left(1-F_{n-1}^k\right)\left(1-\beta F_{n-2}^k\right)\left(1-\beta F_{n+2}^k\right)\Big) \\
& - F_n^k\left(\left(1-F_{n+1}^k\right)\left(1-F_{n+2}^k\right)\left(1-\beta F_{n+3}^k\right)\left(1-\beta F_{n-1}^k\right)\right. \\
& \left. + \left(1-F_{n-1}^k\right)\left(1-F_{n-2}^k\right)\left(1-\beta F_{n-3}^k\right)\left(1-\beta F_{n+1}^k\right)\right)\Big\} \\
+ \frac{\Delta x}{Q^*} \Big\{ & \left(1-F_n^k\right)\left(b_{n-1}^k F_{n-1}^k\left(1-F_{n+1}^k\right)\left(1-\beta F_{n+2}^k\right)\left(1-\beta F_{n-2}^k\right)\right. \\
& - b_{n+1}^k F_{n+1}^k\left(1-F_{n-1}^k\right)\Big)\left(1-\beta F_{n+2}^k\right)\left(1-\beta F_{n-2}^k\right) \\
& - b_n^k F_n^k\left(\left(1-F_{n+1}^k\right)\left(1-F_{n+2}^k\right)\left(1-\beta F_{n+3}^k\right)\left(1-\beta F_{n-1}^k\right)\right. \\
& \left. \left. - \left(1-F_{n-1}^k\right)\left(1-F_{n-2}^k\right)\left(1-\beta F_{n+1}^k\right)\left(1-\beta F_{n-3}^k\right)\right)\right\}.
\end{aligned}
\tag{10}
$$

The model (10) allows for a better examination and understanding of the effect of interference on transmission by examining the network behavior for different values of β. Moreover, in networks that are severely limited by interference, this is a better model of interference than that in network 1.

Network 3 (Directed diffusion routing protocol) We next consider a directed diffusion model in which the routing bias depends on the normalized queue length at neighboring nodes, i.e.,

$$
B_{n,n+1}^k = \frac{1}{2} + \gamma \frac{F_{n-1}^k - F_{n+1}^k}{2}, \quad \gamma \in [-1, 1], \tag{11a}
$$

and interference is according to the interference protocol

$$
1 - I_{n,n\pm1}^k = 1 - F_{n\pm2}^k, \quad \forall n, k. \tag{11b}
$$

The assumption (11a) effectively transmits data *more frequently* in the direction of the neighboring node with the lower probability to transmit. The monotonicity of F then implies data are transmitted more frequently in the direction of the neighboring node with the *smaller* queue. In turn, this protocol seeks to balance the load on the network, reduce the maximum queue, and also reduce the number of unsuccessful transmissions. Since an important characteristic of large networks is energy consumption [18], the energy saving by reducing unsuccessful transmissions is appealing. Inserting (11a) and (11b) into (4) gives

$$
\begin{aligned}
Q_n^{k+1} = Q_n^k + \frac{G_n^k}{Q^*} + \frac{1}{2Q^*} \Big\{ & \left(1-F_n^k\right)\left(F_{n-1}^k\left(1-F_{n+1}^k\right) + F_{n+1}^k\left(1-F_{n-1}^k\right)\right) \\
& - F_n^k\left(\left(1-F_{n+1}^k\right)\left(1-F_{n+2}^k\right) + \left(1-F_{n-1}^k\right)\left(1-F_{n-2}^k\right)\right)\Big\} \\
+ \frac{\gamma}{Q^*} \Big\{ & \left(1-F_n^k\right)\left(\left(\frac{F_{n-2}^k - F_n^k}{2}\right)F_{n-1}^k\left(1-F_{n+1}^k\right) - \left(\frac{F_{n+2}^k - F_n^k}{2}\right)F_{n+1}^k\left(1-F_{n-1}^k\right)\right) \\
& - \left(\frac{F_{n-1}^k - F_{n+1}^k}{2}\right)F_n^k\left(\left(1-F_{n+1}^k\right)\left(1-F_{n+2}^k\right) - \left(1-F_{n-1}^k\right)\left(1-F_{n-2}^k\right)\right)\Big\}.
\end{aligned}
\tag{12}
$$

The significance of the model (12) is that the routing is dependent on the expected normalized queue length of neighboring nodes, which allows for networks to improve routing capabilities and lower expected queue densities in an automated fashion with only local information. For instance, if a few nodes in a small part of the network are doing the majority of the data collection, those nodes must transmit this data to neighbors rapidly so that they can continue to collect data. Such a directed diffusion routing protocol is an alternative to increasing the capacity of the node's queues or quantity of nodes, which are expensive solutions.

3 The continuum modeling approach

In the previous section, we showed how a description of the network and communication protocols leads to a Markov process of normalized queue length vectors, whose expectation then gives rise to a difference equation. In this section, we show under appropriate assumptions that the difference equation can be well approximated by a nonlinear PDE as the number of devices increases. That is, the difference equation is shown to be a discretization for a particular PDE so that, given appropriate smoothness of the expected normalized queue length as the number of nodes tends to infinity and the time step tends to zero, the solution of an appropriate PDE can be made to approximate Q at each of the nodes. The specialized boundary nodes, i.e., sink and wall boundary nodes, yield homogeneous Dirichlet and no-flux boundary conditions, respectively. Some of the tedious details are excluded for clarity and conciseness but, for the model (10) with $\beta = 0$, can be found in [2].

For each of the introduced network models, we take an asymptotic limit of (4) as the number of interior nodes, N, tends to infinity. We let Δx be the distance between neighboring nodes and Δt the difference between transmission times so that

$$x_n = \frac{n}{N+1}\Delta x, \quad n \in \{0, \ldots, N+1\},$$
$$t_k = k\Delta t, \quad k \in \{0, 1, \ldots\}.$$

For the variables obtained in the limit as $\Delta x, \Delta t \to 0$, we use lower-case notation, e.g., $q(t, x)$ and $f(x, q(t, x))$. We assume the scaling $Q^*\Delta t = \Delta x^2$, which is characteristic of diffusion processes and implies a scaling of the time between transmissions that depends on the distance of transmission and the size of a packet relative to Q^*. This choice of scaling is necessary to achieve a nondegenerate limiting PDE and is a consequence of the chosen transmission protocols. Other descriptions of the transmission protocols, e.g., long-range transmission, will require other scalings of time and space and may lead to other types of diffusion, e.g., fractional, nonlocal, and sub/superdiffusion. Further, we assume

$$G_n^k = Q^* g(x)\Delta t,$$

as $\Delta x, \Delta t \to 0$, and that the functions f, b, and g are smooth. The assumption on G guarantees that the number of messages entering the network from external sources is proportional to Δt. We further assume that q is sufficiently smooth so that

$$\begin{aligned} q(t+\Delta t, x) &= q(t, x) + \frac{\partial q}{\partial t}\Delta t + o(\Delta t) \\ q(t, x \pm k\Delta x) &= q(t, x) \pm \frac{\partial q}{\partial x} k\Delta x + \frac{\partial^2 q}{\partial x^2}\frac{k^2\Delta x^2}{2} + o((\Delta x)^2). \end{aligned} \tag{13}$$

Like F, the function f is assumed to satisfy $f(x, 0) = 0$ and $f(x, 1) = 1$ and be monotone in the second variable. For the networks considered in this paper, f, b, and g do not explicitly depend on time, but generalizing to this case is straightforward.

We rearrange (4) and divide by Δt to obtain

$$\begin{aligned} \frac{Q_n^{k+1} - Q_n^k}{\Delta t} = \frac{G_n^k}{Q^*\Delta t} &+ \frac{1}{(\Delta x)^2}\left(1 - F_n^k\right)\left\{ B_{n-1,n}^k F_{n-1}^k \left(1 - I_{n-1,n}^k\right) + B_{n+1,n}^k F_{n+1}^k \left(1 - I_{n+1,n}^k\right) \right\} \\ &- \frac{1}{(\Delta x)^2} F_n^k \left\{ B_{n,n+1}^k \left(1 - F_{n+1}^k\right)\left(1 - I_{n,n+1}^k\right) + B_{n,n-1}^k \left(1 - F_{n-1}^k\right)\left(1 - I_{n,n-1}^k\right) \right\}. \end{aligned} \tag{14}$$

We then insert the Taylor expansions (13) into (14) and take a limit as $\Delta x, \Delta t \to 0$ to obtain a limiting PDE for q. We assume sufficient conditions on $B_{n,n\pm1}^k$ and $I_{n,n\pm1}^k$ so that a limiting PDE exists and takes the form

$$\frac{\partial q}{\partial t} = D(f) + g(x),$$

where $D(f)$ is a nonlinear differential operator so that the resulting PDE is a nonlinear reaction–convection diffusion equation whose time evolution is observed.

We derive in detail the limiting PDE for network 1. Rearranging (8) and dividing by Δt, we have

$$\frac{Q_n^{k+1}-Q_n^k}{\Delta t}=\frac{G_n^k}{Q^*\Delta t}+\frac{c}{2}\frac{F_{n-1}^k-2F_n^k+F_{n+1}^k}{(\Delta x)^2}-2b_0c\left(1-2F_n^k\right)\frac{F_{n+1}^k-F_{n-1}^k}{2\Delta x}.$$

Using the Taylor expansions (13),

$$\frac{\partial q}{\partial t}+o(\Delta t)=\frac{c}{2}\frac{\partial^2 f}{\partial x^2}-2b_0c(1-2f)\frac{\partial f}{\partial x}+g+o((\Delta x)^2),$$

which, taking $\Delta x,\ \Delta t\to 0$, gives[1]

$$\frac{\partial q}{\partial t}=\frac{\partial}{\partial x}\left(\frac{c}{2}\frac{\partial f}{\partial x}-2b_0cf(1-f)\right)+g. \tag{15}$$

When $b_0=0$, $f=q$, and $g=0$, (15) reduces to the classical diffusion equation in one dimension.

Mimicking the previous steps, we find the limiting PDEs for networks 2 and 3 to be

$$\frac{\partial q}{\partial t}=\frac{\partial}{\partial x}\left(\frac{1}{2}(1-f)(1-\beta f)(-5\beta f^2+(3+\beta)f+1)\frac{\partial f}{\partial x}-2bf(1-f)^2(1-\beta f)^2\right)+g \tag{16}$$

and

$$\frac{\partial q}{\partial t}=\frac{\partial}{\partial x}\left(\frac{1}{2}(1-f)(1+3f+4\gamma f-4\gamma f^2)\frac{\partial f}{\partial x}\right)+g, \tag{17}$$

respectively. We remark that the special case of $\beta=0$ in (16) yields the PDE model

$$\frac{\partial q}{\partial t}=\frac{\partial}{\partial x}\left(\frac{1}{2}(1-f)(1+3f)\frac{\partial f}{\partial x}-2bf(1-f)^2\right)+g, \tag{18}$$

which was studied extensively in [2].

3.1 Boundary conditions

We now derive the boundary conditions for network 1 with sink and wall boundary nodes given in Fig. 1. For the sink boundary on the left, we insert (7) into (5) to obtain

$$Q_1^{k+1}=Q_1^k+\frac{G_1^k}{Q^*}-\frac{c}{2Q^*}F_2^k+O(\Delta x).$$

Letting $\Delta x\to 0$ and using the prescribed scaling, we find $f(0,q)=0$, for which the monotonicity of f then implies the homogeneous Dirichlet boundary condition $q(t,0)=0$. Proceeding similarly for the wall boundary on the right, we insert (7) into (6) to obtain

$$Q_1^{k+1}=Q_1^k+\frac{G_1^k}{Q^*}+\frac{c}{2Q^*}\left(F_{N-1}^k-F_N^k\right)+\frac{c}{2Q^*}\left(F_{N-1}^k+F_N^k-2F_{N-1}^kF_N^k\right).$$

Dividing by Δx and then letting $\Delta x\to 0$, we obtain the no-flux condition

$$\frac{c}{2}\frac{\partial f}{\partial x}-2b_0cf(1-f)=0.$$

[1] We have suppressed notation here and throughout the rest of the paper:

$f:=f(x,q),\quad g:=g(x),\ \text{and}\ b:=b(x,q,q').$

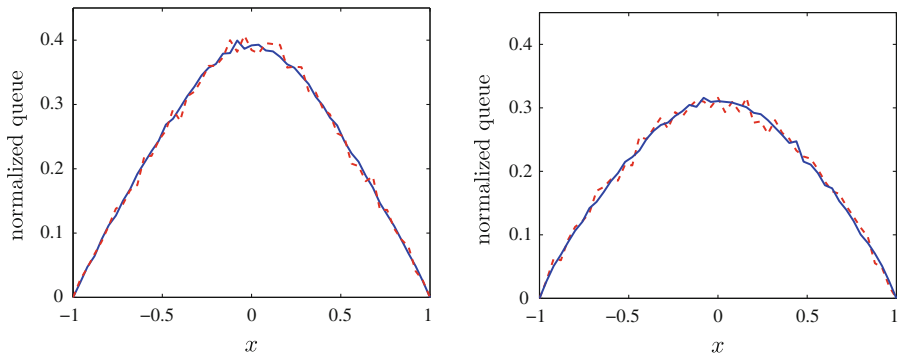

Fig. 2 The ensemble-average normalized queue length computed from simulations of the discrete network with $M = 10$ (*dashed*) and $M = 100$ (*solid*) corresponding to the PDE models (16) (*left*) and (17) (*right*)

For networks 2 and 3, the homogeneous Dirichlet boundary condition can again be derived for the sink boundary node and the no-flux boundary conditions

$$\frac{1}{2}(1-f)(1-\beta f)(-5\beta f^2+(3+\beta)f+1)\frac{\partial f}{\partial x}-2bf(1-f)^2(1-\beta f)^2=0$$

and

$$\frac{1}{2}(1-f)(1+3f+4\gamma f-4\gamma f^2)\frac{\partial f}{\partial x}=0,$$

respectively, for the wall boundary node.

3.2 Comparison of continuum with discrete network models

The derivations of the models (16) and (17) demonstrate that the solution of the PDE continuum models approximates the expected normalized queue length in the corresponding discrete network since the difference equations (10) and (12) were shown to be finite-difference discretizations of the corresponding PDE models. We now present simulation results for the one-dimensional networks (16) and (17) with $\beta = 0.35$ and $\gamma = 1$, respectively. The ensemble average of normalized queue lengths from the simulations is compared with the normalized queue length from the limiting PDE model.

We consider a network of $N + 2 = 51$ nodes uniformly placed on the interval $[-1, 1]$, where the two nodes on the boundary are sinks. The network parameters are described in terms of the PDE model. We consider an initial normalized queue length of $q(0, x) = 0.5\exp(-5x^2)$, data are collected according to $g(x) = 0.8\exp(-5x^2)$, $f(x, q) = q$, and there is no convection, i.e., $b = 0$. A maximum of $Q^* = 150$ messages may be stored in each queue. The ensemble average of $M = 10$ and $M = 100$ simultaneous network simulations after $T = 50{,}000$ time steps are shown in Fig. 2. The numerical solutions of the PDE are not plotted because they are nearly indistinguishable from the $M = 100$ simulation results; i.e., the solutions of the PDEs capture the expected normalized queue length. Approximating solutions to these PDEs via finite-element methods is performed in seconds, while these simulations required over an hour each.

4 Network and continuum models in two dimensions

For conciseness, we condense the discussion of network models in two spatial dimensions. Transmission and interference protocols are similar to those in one dimension, except there are four directions to consider: north, south,

east, and west. Nodes are denoted with the ordered pair (n, j) to give the x and y positions. Also, $B^k_{n,n+1,j,j}$ is the probability of transmitting from node (n, j) to node $(n+1, j)$, whereas $1 - I^k_{n,n+1,j,j}$ is the probability that this transmission is not interfered with. The expectation of the Markov process is given by

$$Q^{k+1}_{n,j} = Q^k_{n,j} + \frac{G^k_{n,j}}{Q^*} + \frac{1}{Q^*} \sum_{r=\pm 1} \sum_{s=\pm 1} \left(A^k_{n,n+r,j,j} + A^k_{n,n,j,j+s} \right),$$

where, for example,

$$\begin{aligned} A^k_{n,n+1,j,j} = &\left(1 - F^k_{n,j}\right) B^k_{n+1,n,j,j} F^k_{n+1,j} \left(1 - I^k_{n+1,n,j,j}\right) \\ &- F^k_{n,j} B^k_{n,n+1,j,j} \left(1 - F^k_{n+1,j}\right) \left(1 - I^k_{n,n+1,j,j}\right). \end{aligned}$$

We only present the two-dimensional analogs of (16) and (17). Homogeneous Dirichlet and no-flux boundary conditions can be derived for sink and wall boundary nodes, respectively.

Network 2 The two-step interference protocol model incorporates interference probabilities from all nodes that are within a two-node radius of the intended receiver. Thus, diagonally neighboring nodes also provide interference, which we model by assigning a probability α of a diagonally neighboring node interfering when transmitting. To reflect that interference decreases with distance, $\alpha \geq \beta$. For this model, we define

$$B^k_{n,n+1,j,j} = \frac{1}{4} + \mathbf{b}^k_{n,j} \cdot \mathbf{e}_1 \Delta x \quad \text{and} \quad B^k_{n,n,j,j+1} = \frac{1}{4} + \mathbf{b}^k_{n,j} \cdot \mathbf{e}_2 \Delta x,$$

where $\mathbf{e}_i$ is the ith standard basis vector. To model interference, we assume

$$\begin{aligned} 1 - I^k_{n,n\pm1,j,j} = &\left(1 - F^k_{n\pm2,j}\right) \left(1 - F^k_{n\pm1,j-1}\right) \left(1 - F^k_{n\pm1,j+1}\right) \\ &\times \left(1 - \beta F^k_{n\mp1,j}\right) \left(1 - \beta F^k_{n\pm3,j}\right) \left(1 - \beta F^k_{n\pm1,j-1}\right) \left(1 - \beta F^k_{n\pm1,j+2}\right) \\ &\times \left(1 - \alpha F^k_{n,j-1}\right) \left(1 - \alpha F^k_{n,j+1}\right) \left(1 - \alpha F^k_{n\pm2,j-1}\right) \left(1 - \alpha F^k_{n\pm2,j+1}\right) \end{aligned}$$

and similarly for $1 - I^k_{n,n,j,j\pm1}$. These assumptions give rise to the PDE model

$$\frac{\partial q}{\partial t} = \nabla \cdot \left[\frac{1}{4}(1-f)^3(1-\alpha f)^3(1-\beta f)^3 \eta \nabla f - 2\mathbf{b} f (1-f)^4 (1-\alpha f)^4 (1-\beta f)^4 \right] + g, \tag{19}$$

where

$$\eta := 13\alpha\beta f^3 - (9\alpha + 9\beta + 7\alpha\beta) f^2 + (3\alpha + 3\beta + 5) f + 1.$$

As in the one-dimensional case, choosing $\alpha = \beta = 0$ yields the PDE model

$$\frac{\partial q}{\partial t} = \nabla \cdot \left[\frac{1}{4}(1-f)^3(1+5f) \nabla f - 2\mathbf{b} f (1-f)^4 \right] + g, \tag{20}$$

which was studied extensively in [2].

Network 3 To incorporate a routing bias that transmits data more frequently to neighbors with lower queues, we define

$$B^k_{n,n+1,j,j} = \frac{1}{4} + \gamma \frac{F^k_{n-1,j} - F^k_{n+1,j}}{2} \quad \text{and} \quad B^k_{n,n,j,j+1} = \frac{1}{4} + \gamma \frac{F^k_{n,j-1} - F^k_{n,j+1}}{2}, \quad \gamma \in [-1/2, 1/2].$$

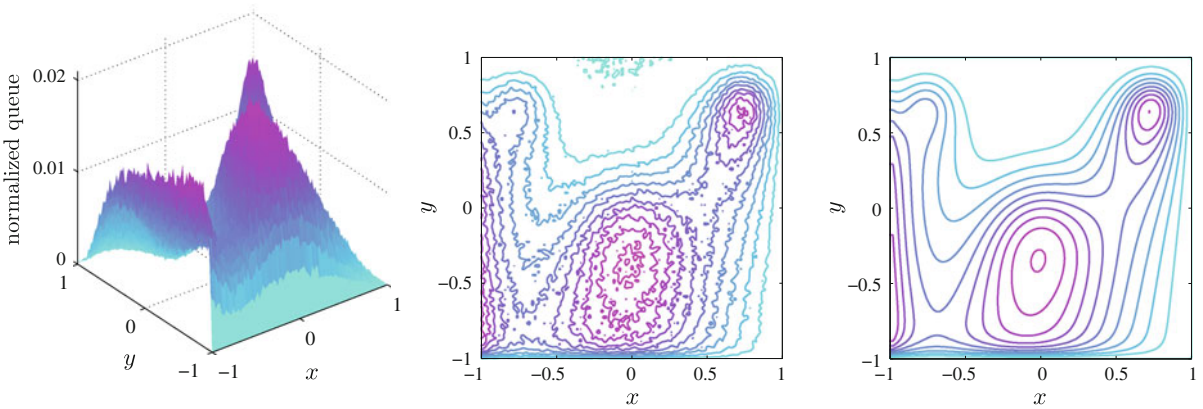

(a) **(b)** **(c)**

Fig. 3 Surface (**a**) and contour (**b**) plots of expected normalized queue length computed from the simulations. Contour plot (**c**) of the expected normalized queue length computed from the corresponding PDE

To model interference, we assume

$$1 - I^k_{n,n\pm1,j,j} = \left(1 - F^k_{n\pm2,j}\right)\left(1 - F^k_{n\pm1,j-1}\right)\left(1 - F^k_{n\pm1,j+1}\right)$$

and similarly for $1 - I^k_{n,n,j,j\pm1}$. These assumptions give rise to the PDE model

$$\frac{\partial q}{\partial t} = \nabla \cdot \left[\frac{1}{4}(1-f)^3(1+5f+8\gamma f-8\gamma f^2)\nabla f\right] + g. \tag{21}$$

To demonstrate that the solution of the PDE models capture the expected normalized queue length in the network, we consider (20), convection $\mathbf{b} = (1,\ \ 5)^T$, data collection governed by

$$g(x,y) = 0.3\exp\left(-50(x+0.75)^2 - 50(y+0.75)^2\right) + 0.6\exp\left(-50(x-0.75)^2 - 50(y-0.75)^2\right) + 0.2\exp\left(-10x^2 - 10y^2\right),$$

$q(0,x,y) = 0.03g(x,y)$, $N = 99$, $Q^* = 100$, $M = 500$, $T = 125{,}000$, which is equivalent to about 0.5 s in the continuum model, wall boundaries on the north and west boundaries, and sink boundaries elsewhere. Solving the PDE model takes under a minute while completing the simulation takes several days,[2] which makes optimization and design studies computationally impractical with simulation techniques (Fig. 3).

5 Network design studies

In this section, we use the PDE models to study network properties, investigate the effects of various parameters on the efficiency of the network, and consider practical network design problems. The speed at which solutions of the PDE models are obtained makes optimization and design studies possible. Such studies play a critical role in the design and implementation of real wireless networks.

For $g > 0$, the network must transmit packets through the network sufficiently rapidly so that $q < 1$. In the absence of convection, the models have similar characteristics. The diffusion coefficients of the PDE models (16), (18), and (17),

[2] These were performed on the same computer and took roughly 44.45 s and 12.46 days, respectively.

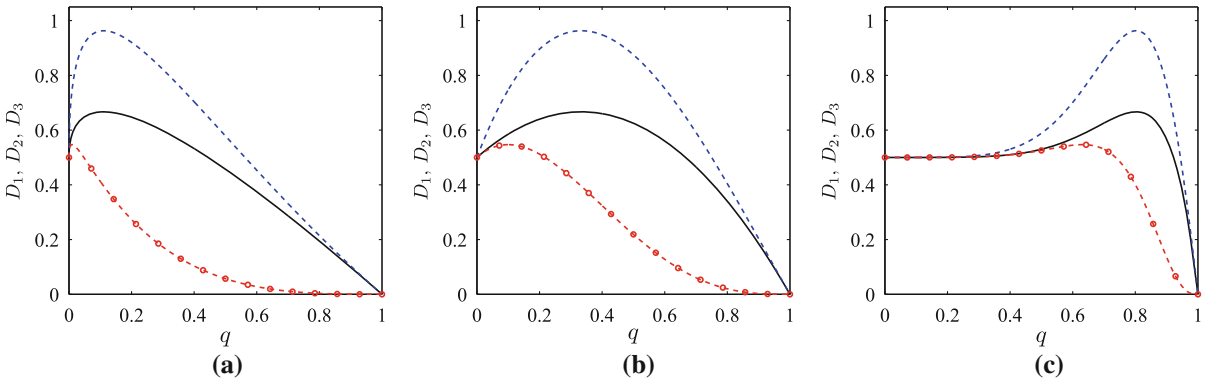

Fig. 4 Diffusion coefficients D_1 with $\beta = 1$ (*marked*), D_2 (*solid*), and D_3 with $\gamma = 1$ (*dashed*) for (**a**) $f(x, q) = q^{0.5}$, (**b**) $f(x, q) = q$, and (**c**) $f(x, q) = q^5$

$$D_1 = \frac{1}{2}(1-f)(1-\beta f)(-5\beta f^2 + (3+\beta)f + 1), \quad D_2 = \frac{1}{2}(1-f)(1+3f), \quad \text{and}$$
$$D_3 = \frac{1}{2}(1-f)(1+3f+4\gamma f - 4\gamma f^2), \tag{22}$$

respectively, provide insight into how efficiently the transmission protocol moves data through the network. If $q = 0$, $D_i = \frac{1}{2}$ and, if $q = 1$, $D_i = 0$. The behavior of D_i for $q \in (0, 1)$ depends on f, β, and γ. In Fig. 4, we plot the diffusion coefficients in (22) with different choices of f. For each value of $f(x, q)$, the diffusion coefficient increases as γ increases and decreases as β increases. These are expected since the directed diffusion routing protocol reduces the number of unsuccessful transmissions, hence increases diffusion, and the addition of interference does the opposite.

For $\beta > 0$, the diffusion coefficient D_1 becomes convex for sufficiently large values of q. For example, when $\beta = 1$ and $f(x, q) = q = 0.4$, there is an inflection point at $q = 0.4$. This causes a dramatic reduction in the diffusion coefficient for large queue values, suggesting that interference-sensitive networks are susceptible to failure under heavy loading, since large queues lead to drastically slower diffusion, leading to larger queues, and so on.

The following examples all consider two-dimensional networks on $[-1, 1] \times [-1, 1]$ with $f(x, y, q) = q$ and no convection. Each example demonstrates the capability of the continuum models for optimization and design studies that simulation-based algorithms are limited from.

*Example 5.1 (*Network failure under heavy loading*)* We consider a network with sink boundary nodes on the west boundary for $y \in [-1, -0.8]$ and the south boundary for $x \in [-0.8, -0.4] \cup [0.4, 1]$ and wall boundary nodes elsewhere. Data are collected according to

$$g(x, y) = \lambda\left(\sum_{a,b\in\{0.4,0.8\}}\sum \exp\Big[-100(x+a)^2 - 100(y-b)^2\Big]\right), \tag{23}$$

for a given λ. Thus, data are collected in four small regions, while the rest of the network must relay data through the network. We begin by choosing $\lambda = 0.6$ and note that increasing λ represents increasing the data collection in the network. For the models (19) with $\alpha = 0.35$ and $\beta = 0.2$, (20), and (21) with $\gamma = 0.5$, we compare throughput,

$$\iint_{\Omega}\left(g(x, y) - \frac{\partial q(t, x, y)}{\partial t}\right)\mathrm{d}x\mathrm{d}y,$$

and the maximum queue values for $t \in [0, 30]$. As q tends to a steady-state profile, $\partial q/\partial t \to 0$ and the throughput converges to the total input provided by the source. Network designs that require less time for the throughput to

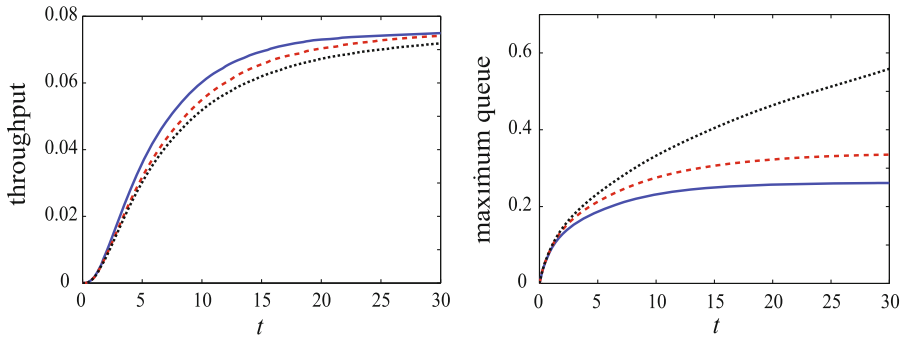

Fig. 5 Plots of throughput and the maximum queue in the network for the models (19) with $\alpha = 0.35$ and $\beta = 0.2$ (*dotted*), (20) (*dashed*), and (21) with $\gamma = 0.5$ (*solid*)

reach a specified value are desired. The results are shown in Fig. 5. Since the maximum normalized queue length in each model is different, we can infer that the steady-state solutions of the models are different. Thus, not only do the networks behave differently in the transient times but the equilibrium behavior is different as well. The directed diffusion model (21) reaches a desired throughput more quickly, suggesting the network is more efficient, and allows the network to maintain a low maximum queue. The model (19), however, reaches a desired throughput much more slowly, causing the maximum queue in the network to be large as well.

We now investigate the "failure" of a network under heavy loading, e.g., choosing λ sufficiently large, which requires ironing out a few subtle details. In the network simulations, there is a nonzero probability that a particular node at any time will reach its capacity, Q^*. Since we are interested instead in modeling the *expected* normalized queue length, we allow nodes to become full with additional data being stored as well, e.g., in a secondary backup queue. We must exercise caution here because the continuum modeling approach is only valid when the expected normalized queue length q is less than one; e.g., as q approaches one, solutions of the PDE models will blow up. This is tantamount to, on average, nodes in the discrete networks being overfull. Again, the case $q \geq 1$ is not in the regime we have considered in the modeling approach and the continuum model is no longer valid. It is outside of the scope of this paper, but an entirely different and interesting question concerns the probability of a particular network being overfull.

Again referring to Fig. 5, the maximum queue in the model (19) is substantially larger than in the other two models. In fact, increasing λ to 0.7 in (23) causes the network modeled by (19) to fail; i.e., the expected normalized queue length is above one so that the queues are full and data can no longer be collected. Further, increasing λ to 0.93 causes that of (20) to also fail. However, as demonstrated in Fig. 6, the directed diffusion model (21) performs very well even for large λ and keeps the maximum queue below half of its capacity. In Fig. 7 we plot contours of solutions to (19) and (21). The interference-sensitive network is unable to move data sufficiently fast from the area of the network that is sensing. As a result, the queues become full in that region, unlike the directed diffusion model which efficiently spreads data to the nonsensing regions of the network. A directed diffusion routing bias in the network allows for much more data to be collected without overfilling the queues. From a design perspective, understanding these characteristics is critical.

Example 5.2 (Analysis of throughput) We investigate throughput of the network model (19) for various α, β. We choose sink boundaries on the south boundary, west boundary for $y \in [0.2, 0.6]$, and the north boundary for $x \in [-0.6, -0.2]$ and wall boundaries elsewhere. The network begins empty of data, i.e., $q(0, x, y) = 0$, and data are collected according to

$$g(x, y) = 0.05 + \frac{5}{2\pi} \exp\left(-100(x - 0.5)^2 - 100(y - 0.25)^2\right).$$

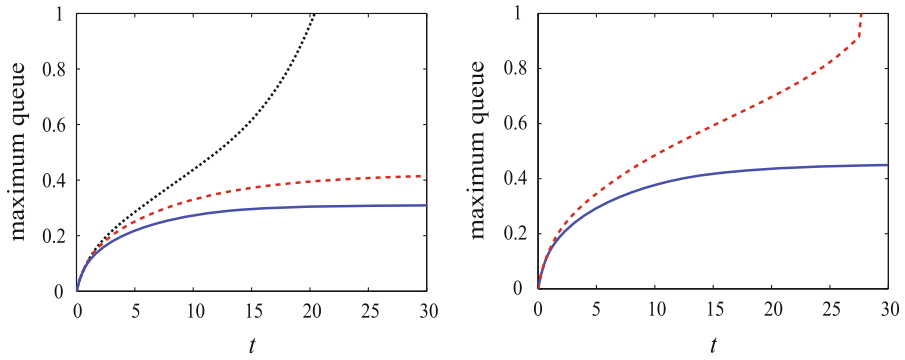

Fig. 6 Plots of the maximum queue for $\lambda = 0.7$ (*left*) and $\lambda = 0.93$ (*right*) for the models (19) (*dotted*), (20) (*dashed*), and (21) (*solid*). Model (19) is not plotted on the *right*

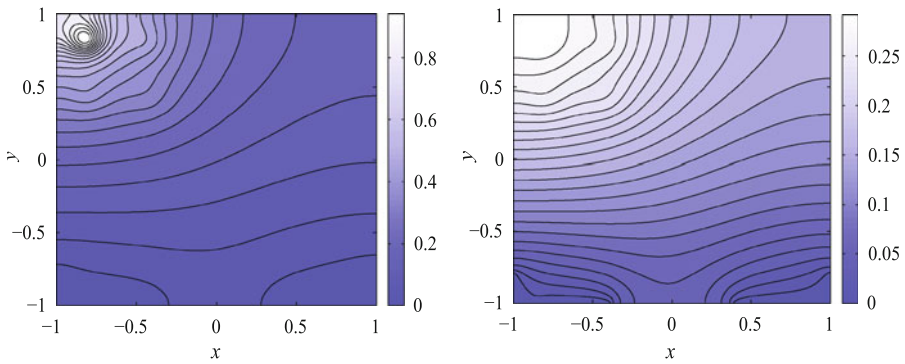

Fig. 7 Contour plots at $t = 20.25$ (before failure) with $\lambda = 0.7$ for the models (19) (*left*) and (21) (*right*)

The throughput is monitored and the collection of data is turned off, $g = 0$, when the throughput reaches 98 % of its maximum value, i.e., 98 % of the throughput at steady state,

$$0.98 \iint_{\Omega} g(x, y)\, \mathrm{d}x\mathrm{d}y = 0.2205.$$

After forcing is removed, we monitor throughput as data are removed from the network. The results are given in Fig. 8 for $\alpha, \beta = 0$, $\alpha, \beta = 0.2$, and $\alpha, \beta = 0.4$. Increasing α and β increases the time until the forcing is shut off, i.e., the time required to reach the desired throughput. This implies that data are not being transmitted out of the network as quickly, due to inefficient communication, for large α, β.

Consider the same network with $g = 0$ and an initial condition

$$q(0, x, y) = \frac{5}{2\pi} \exp\Big(-100(x - 0.5)^2 - 100(y - 0.25)^2\Big).$$

The maximum queue throughout the network is monitored. For large α, β, the maximum queue decays much more slowly, due to the increased interference. This again suggests that networks that are sensitive to interference are unable to efficiently move large quantities of data, e.g., arising from very localized sensing, through the network and, consequently, are susceptible to failure. These results are plotted in Fig. 9.

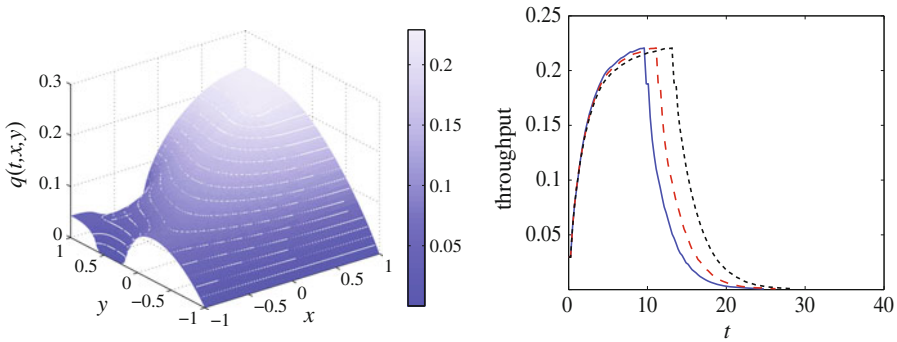

Fig. 8 The steady-state profile for the described network with $\alpha, \beta = 0$ (*left*). Throughput histories (*right*) for $\alpha, \beta = 0$ (*solid*), $\alpha, \beta = 0.2$ (*dashed*), and $\alpha, \beta = 0.4$ (*dotted*)

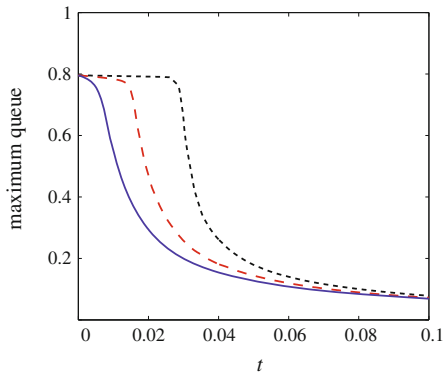

Fig. 9 Maximum queue histories for a network with an initial normalized queue length but no data collection for $\alpha, \beta = 0$ (*solid*), $\alpha, \beta = 0.2$ (*dashed*), and $\alpha, \beta = 0.4$ (*dotted*)

6 Conclusions

Continuum models of large networks offer an approach for performing optimization and design studies, which are tools that are not computationally tractable using direct simulation of the networks alone. In this paper, we extend the modeling approach in [2] to analyze effects of routing protocols and interference limitations. The solutions of the resulting continuum models capture the expected behavior of their corresponding discrete networks, while taking minimal time to approximate numerically. This computational saving allows for optimization, performance, and design studies, which are computationally infeasible using simulations of the discrete networks. This gives a fast and powerful tool to aid the design of large networks. This modeling approach has been presented in sufficient generality to allow for networks with a wide range of routing protocols and communication limitations or enhancements.

Acknowledgments This material is based upon work supported by the National Science Foundation under grants ECCS-0700559, DGE-0221595003, MSPA-CSE-0434354, DMS-0707037, DMS-1007543, and DMS-1016441. The first author was supported in part by the National Science Foundation through the Statistical and Applied Mathematical Sciences Institute (SAMSI), grant DMS-0635449.

References

1. Chiasserini CF, Gaeta R, Garetto M, Gribaudo M, Manini D, Sereno M (2007) Fluid models for large-scale wireless sensor networks. Perform Eval 64(7–8):715–736
2. Chong EKP, Estep D, Hannig J (2007) Continuum modeling of large networks. Int J Numer Model Electron Netw Devices Fields 21(3):169–186
3. Hart JK, Martinez K (2006) Environmental sensor networks: a revolution in the earth system science? Earth-Sci Rev 78(3–4): 177–191

4. Estrin D, Govindan R, Heidemann J, Kumar S (1999) Next century challenges: scalable coordination in sensor networks. In: Proceedings of the 5th annual ACM/IEEE international conference on mobile computing and networking. ACM, New York, pp 263–270
5. Lees JM, Johnson JB, Ruiz M, Troncoso L, Welsh M (2008) Reventador volcano 2005: eruptive activity inferred from seismo-acoustic observation. J Volcanol Geotherm Res 176(1):179–190
6. Werner-Allen G, Dawson-Haggerty S, Welsh M (2008) Lance: optimizing high-resolution signal collection in wireless sensor networks. In: Proceedings of the 6th ACM conference on embedded network sensor systems. ACM, New York, pp 169–182
7. Tolle G, Polastre J, Szewczyk R, Turner N, Tu K, Buonadonna P, Burgess S, Gay D, Hong W, Dawson T, Culler D (2005) A macroscope in the redwoods. In: Proceedings of the 3rd international conference on embedded networked sensor systems. ACM, New York, p 63
8. Akyildiz IF, Su W, Sankarasubramaniam Y, Cayirci E (2002) Wireless sensor networks: a survey. Comput Netw 38(4):393–422
9. Martinez K, Hart JK, Ong R (2004) Environmental sensor networks. Computer 37(8):50–56
10. Gamal HE (2005) On the scaling laws of dense wireless sensor networks: the data gathering channel. IEEE Trans Inf Theory 51(3):1229–1234
11. Toumpis S, Tassiulas L (2005) Packetostatics: deployment of massively dense sensor networks as an electrostatics problem. In: INFOCOM 2005. 24th Annual joint conference of the IEEE computer and communications societies. Proceedings IEEE, vol 4. IEEE, pp 2290–2301
12. Toumpis S, Tassiulas L (2006) Optimal deployment of large wireless sensor networks. IEEE Trans Inf Theory 52(7):2935–2953
13. Ganesan D, Krishnamachari B, Woo A, Culler D, Estrin D, Wicker S (2002) Complex behavior at scale: an experimental study of low-power wireless sensor networks. Technical report, Citeseer
14. Gupta P, Kumar PR (2000) The capacity of wireless networks. IEEE Trans Inf Theory 46(2):388–404
15. Herdtner JD, Chong EKP (2005) Throughput-storage tradeoff in ad hoc networks. In: Proceedings IEEE INFOCOM 2005. 24th Annual joint conference of the IEEE computer and communications societies, vol 4
16. Li J, Blake C, De Couto DSJ, Lee HI, Morris R (2001) Capacity of ad hoc wireless networks. In: Proceedings of the 7th annual international conference on mobile computing and networking. ACM, New York, p 69
17. Xie LL, Kumar PR (2004) A network information theory for wireless communication: scaling laws and optimal operation. IEEE Trans Inf Theory 50(5):748–767
18. Jain K, Padhye J, Padmanabhan VN, Qiu L (2005) Impact of interference on multi-hop wireless network performance. Wirel Netw 11(4):471–487
19. Klein DJ, Hespanha J, Madhow U (2010) A reaction-diffusion model for epidemic routing in sparsely connected MANETs. In: INFOCOM, 2010 proceedings IEEE. IEEE, pp 1–9
20. Kalantari M, Shayman M (2004) Energy efficient routing in wireless sensor networks. In: Proceedings of conference on information sciences and systems, Citeseer
21. Kalantari M, Shayman M (2004) Routing in wireless ad hoc networks by analogy to electrostatic theory. In: 2004 IEEE international conference on communications, vol 7. IEEE, pp 4028–4033
22. Kalantari M, Haghpanahi M, Shayman M (2008) A p-norm flow optimization problem in dense wireless sensor networks. In: INFOCOM 2008. The 27th conference on computer communications. IEEE, pp 341–345
23. Zhang Y, Chong EKP, Hannig J, Estep D (2010) On continuum limits of Markov chains and network modeling. In: 2010 49th IEEE conference on decision and control (CDC), pp 6779–6784. IEEE